The university of Tartu
Faculty of Physics & Chemistry
Institute of Theoretical Physics

Running of Low-Energy Neutrino Masses and Mixing Angles in the Minimal Supersymmetric Standard Model

KRISTJAN KANNIKE

Master thesis

Supervisors: Martti Raidal, Ph.D.
Rein Saar, Ph.D.

Tartu, 2005

Contents

1. Introduction

In the Standard Model of particle physics, the neutrinos are massless particles of spin 1/2, totally unlike the other fermions such as the charged leptons (e, μ, τ) or quarks. Though experimental evidence was lacking at the time, the possibility of massive neutrinos was already considered fifty years ago.[1]

The discovery of neutrino oscillations in recent years – implying very small but non-zero neutrino masses – is the first experimental indication of physics beyond the Standard Model (SM). Neutrino flavour eigenstates (of which electron and muon neutrinos can be experimentally detected) are not the same as their mass eigenstates, but superpositions of these. Thus the probability to find electron neutrinos in a neutrino stream coming e.g. from the Sun, oscillates with time, explaining the once mysterious deficit of solar electron neutrinos. (The Super-Kamiokande collaboration [2] was notably the first statistically unambiguous experiment to present strong evidence for atmospheric neutrino oscillations, showing that the deficit in neutrino flux depends on the path length and energy of neutrinos as expected. The data from Sudbury Neutrino Observatory [3] [4] support the Large Mixing Angle (LMA) solution.)

Unlike the quark mixing matrix, its lepton counterpart $U_{\rm MNS}$ that transforms neutrino mass eigenstates into flavour eigenstates has two large mixing angles. The differences between squared neutrino masses have been determined experimentally. Still, the overall mass scale (with the exception of an upper limit) and the values of the CP-violating phases in the neutrino mixing matrix are not yet known.

In the seesaw mechanism [5] [6] [7] [8] [9], SM is extended with three right-handed neutrino singlets that generate neutrino masses m_ν via their Yukawa couplings Y_ν. Due to the lack of protective symmetries,

[1] For a comprehensible overview of neutrino physics see [1].

the singlets are very massive, accounting for the smallness of light neutrino masses:

$$m_\nu = \frac{v^2}{2} Y_\nu^T M^{-1} Y_\nu,$$

which results from integrating out the singlets with mass matrix M.

To stabilize the electroweak scale against radiative corrections, especially to cancel a quadratically divergent contribution to the Higgs mass from neutrino singlets, the model is supersymmetrized, giving the Minimal Supersymmetric Standard Model (MSSM) with heavy neutrinos. The relevant RGEs were derived in [10] [11] [12].

As the seesaw mechanism operates on a high mass scale, neutrino mass matrix at the experimentally accessible electroweak scale must be calculated by solving renormalization group equations (RGEs) that give quantum corrections for neutrino masses and mixing angles.

The structure of mixing angles and masses, evolved to the GUT scale, can give rise to interesting possibilities in the model building. In cosmology, the leptogenesis mechanism [13] to generate the observed baryon asymmetry in the universe can be based on the out-of-equilibrium decay of the very same heavy neutrino singlets that give rise to neutrino mass via the seesaw mechanism. The singlets are expected to have masses a few magnitude below the gauge unification scale, and the neutrino mixing parameters have to be evolved there by RGE running.

In this thesis, we study the renormalization group running of neutrino mixing angles and masses from experimentally measured values to the gauge coupling unification scale.

The numerical results of RGE running are compared to the analytical approximations by Antusch *et al.* [14].

Changes in neutrino mass hierarchy are studied.

2. Generation of Neutrino Masses

2.1. **Effective Theories from Integrating Out Singlet Neutrinos.** Integrating out the heavy neutrino singlets with masses $M_1 \leq M_2 \leq M_3$ one-by-one results in effective theories, each valid in a respective energy interval between mass thresholds [12].

In the MSSM, the gauge singlet Weyl spinors ν^{C_i}, corresponding to the right-handed Dirac spinors N_R^i of the SM, and their superpartners are components of the chiral superfields $\mathbb{v}^{\mathrm{C}_i}$. The terms of the superpotential containing the superfields are

$$\mathscr{W}_{(\mathrm{N})} = \frac{1}{2}\mathbb{v}^{\mathrm{C}_i} M_{ij} \mathbb{v}^{\mathrm{C}_j} + (Y_\nu)_{if} \mathbb{v}^{\mathrm{C}_i} \mathbb{h}_a^{(2)} (\varepsilon^T)^{ab} \mathbb{l}_b^f + \mathrm{h.c.}, \tag{2.1}$$

where $\mathbb{l}^f$ and $\mathbb{h}^2$ are the chiral superfields that contain the leptonic $\mathrm{SU}(2)_\mathrm{L}$-doublets and the Higgs doublet with weak hypercharge $+1/2$. ε is the Levi-Civita tensor in 2 dimensions, and $a, b, c, d \in \{1, 2\}$ are SU(2) indices.

The Higgs doublet superfield $\mathbb{h}^{(1)}$ with weak hypercharge $-1/2$ is tied to the Yukawa couplings of the $\mathrm{SU}(2)_\mathrm{L}$-singlet superfields $\mathbb{e}^\mathrm{C}$ and $\mathbb{d}^\mathrm{C}$ that contains the charged leptons and down-type quarks, while $\mathbb{h}^{(2)}$ is coupled to $\mathbb{v}^\mathrm{C}$ and the superfield $\mathbb{u}^\mathrm{C}$ containing the up-type quarks. The part of the superpotential describing the remaining Yukawa interactions is

$$\begin{aligned}\mathscr{W}_Y^{\mathrm{MSSM}} = (Y_e)_{gf} \mathbb{e}^{\mathrm{C}_g} \mathbb{h}_a^{(1)} \varepsilon^{ab} \mathbb{l}_b^f + (Y_d)_{gf} \mathbb{d}^{\mathrm{C}_g} \mathbb{h}_a^{(1)} \varepsilon^{ab} \mathbb{q}_b^f \\ + (Y_u)_{gf} \mathbb{u}^{\mathrm{C}_g} \mathbb{h}_a^{(2)} (\varepsilon^T)^{ab} \mathbb{q}_b^f,\end{aligned} \tag{2.2}$$

where $\mathbb{q}$ is the quark doublet superfield.

By integrating out all singlets in the MSSM, the dimension 5 operator that gives Majorana masses to neutrinos is obtained: it is the F-term of

$$\mathscr{W}_\kappa^{\mathrm{MSSM}} = -\frac{1}{4}\kappa_{gf} \mathbb{l}_c^g \varepsilon^{cd} \mathbb{h}_d^{(2)} \mathbb{l}_b^f \varepsilon^{ba} \mathbb{h}_a^{(2)} + \mathrm{h.c.} \tag{2.3}$$

After electroweak symmetry breaking, the light neutrino mass matrix is given by the seesaw mechanism

$$m_\nu = \frac{v^2}{2} Y_\nu^T M^{-1} Y_\nu, \tag{2.4}$$

where m_ν is proportional to the effective coupling κ:

$$m_\nu = \frac{v^2 \sin^2\beta}{2}\,\kappa. \tag{2.5}$$

2.2. **Matching of Effective Theories.** In general, heavy neutrino masses – eigenvalues of the singlet mass matrix M – are non-degenerate: $M_1 \leq M_2 \leq M_3$. At each mass threshold M_n, the corresponding neutrino singlet superfield $\mathbb{v}^n$ is integrated out, giving rise to an effective theory each valid in the energy interval below the singlet and above the next mass scale [12].[2]

Let us work in the basis where the singlet mass matrix M is diagonal. (To transform Y_ν to the same base, $Y_\nu \to U_M^* Y_\nu$, where U_M is the matrix that diagonalizes M.)

Above M_3, the highest mass threshold, Y_ν is a 3×3 matrix that is generally non-zero. At each mass threshold M_n a row in $\overset{(n)}{Y}_\nu$, beginning from the last one, is set to zero. The accent (n) on $\overset{(n)}{Y}_\nu$ shows the number of non-zero rows. Similarly, at each M_n, that mass is removed from M. (E.g. at M_3, the element $M_{33}(= M_3)$ of the singlet mass matrix is set to zero).

The tree-level matching condition for the effective coupling constant at each heavy mass eigenvalue is

$$\overset{(n)}{\kappa}_{gf}|_{M_n} = \overset{(n+1)}{\kappa}_{gf}|_{M_n} + \overset{(n+1)}{(Y_\nu^T)}_{gn} \overset{(n+1)}{M^{(-1)}} \overset{(n+1)}{(Y_\nu)}_{gn}|_{M_n}. \tag{2.6}$$

(No sum over n is implied. $M^{(-1)}$ is the Moore-Penrose *pseudo*inverse of the matrix M. E.g. at M_2, the matrix $\overset{(1)}{M}{}^{(-1)}$ is zero, except for

[2]Note that here the "point of view" is *descending* the energy scale from a more fundamental theory, in contrast to our calculations where we evolve the parametres from the electroweak up to the GUT scale.

the element $(\overset{(1)}{M}{}^{(-1)})_{11} = 1/M_1$. Above M_3 where M is invertible, the pseudoinverse reduces to the standard matrix inverse.)

Below M_1, the lowest threshold, $Y_\nu^T \overset{(0)}{M}{}^{(-1)} Y_\nu = 0$, and the running of the mixing angles, phases, and masses comes from the running of κ_{gf} alone. Above the highest threshold, $\kappa_{gf} = 0$, and only the running of Y_ν and M contributes via the seesaw mechanism (2.4) to the running of neutrino parametres. Note that in general the masses and the mixing matrix have to be calculated from the combination

$$\kappa' = \kappa + 2 Y_\nu^T \overset{(n)}{M}{}^{(-1)} Y_\nu. \tag{2.7}$$

2.3. **RGEs for Neutrino Mass Matrix Running.** The renormalisation group equations are differential equations in the form

$$\overset{(n)}{\beta}_\kappa = \mu \frac{\mathrm{d}\overset{(n)}{\kappa}_{gf}}{\mathrm{d}\mu}, \tag{2.8}$$

where μ is the renormalization scale.

For the the MSSM with additional chiral superfields including heavy neutrino singlets, the β-function for the effective coupling constant (proportional to the neutrino mass matrix) below the nth threshold is given by

$$\begin{aligned} 16\pi^2 \overset{(n)}{\beta}_\kappa = {} & (Y_e^\dagger Y_e)^T \overset{(n)}{\kappa} + \overset{(n)}{\kappa} (Y_e^\dagger Y_e) + (\overset{(n)}{Y}{}_\nu^\dagger \overset{(n)}{Y}_\nu)^T \overset{(n)}{\kappa} \\ & + \overset{(n)}{\kappa} (\overset{(n)}{Y}{}_\nu^\dagger \overset{(n)}{Y}_\nu) + 2\,\mathrm{Tr}\, \overset{(n)}{Y}{}_\nu^\dagger \overset{(n)}{Y}_\nu) \overset{(n)}{\kappa} + 6\,\mathrm{Tr}\, \overset{(n)}{Y}{}_u^\dagger \overset{(n)}{Y}_u) \overset{(n)}{\kappa} - 2 g_1^2 \overset{(n)}{\kappa} - 6 g_1^2 \overset{(n)}{\kappa}. \end{aligned} \tag{2.9}$$

the β-function for the singlet Yukawa matrix $\overset{(n)}{\beta}_{Y_\nu}$ is

$$\overset{(n)}{\beta}_{Y_\nu} = \overset{(n)}{\beta}_{Y_\nu} \left[3 Y_\nu^\dagger Y_\nu + Y_e^\dagger Y_e + \mathrm{Tr}\,(Y_\nu^\dagger Y_\nu) + 3\,\mathrm{Tr}\,(Y_u^\dagger Y_u) - g_1^2 - 3 g_2^2 \right], \tag{2.10}$$

and the β-function for the Majorana mass matrix M of the heavy singlet neutrinos is given by

$$\overset{(n)}{\beta}_M = 2 (\overset{(n)}{Y}_\nu \overset{(n)}{Y}{}_\nu^\dagger) \overset{(n)}{M} + 2 \overset{(n)}{M} (\overset{(n)}{Y}_\nu \overset{(n)}{Y}{}_\nu^\dagger)^T. \tag{2.11}$$

These RGE-s were derived in [10] [11] [12].

The β-functions for the gauge couplings and for the Yukawa couplings of the quarks and charged leptons are not given here. They are the same as in the extended SM or MSSM [15], if one substitutes $\overset{(n)}{Y}_\nu$ for Y_ν [12].

2.4. **Analytical Approximations.** Analytical approximations to RG running of mixing angles, phases and masses were derived in [14]. The RGE in the MSSM for the composite matrix m'_ν that is proportional to κ' (2.7) is

$$16\pi^2 \frac{\mathrm{d}m'_\nu}{\mathrm{d}t} = (Y_e^\dagger Y_e + Y_\nu^\dagger Y_\nu)^T m'_\nu + m'_\nu((Y_e^\dagger Y_e + Y_\nu^\dagger Y_\nu)) + \bar{\alpha} m'_\nu \tag{2.12}$$

with $t = \ln(\mu/\mu_0)$, and

$$\bar{\alpha} = -\frac{6}{5} g_1^2 - 6 g_2^2 + \mathrm{Tr}\, Y_\nu^\dagger Y_\nu + 3 Y_u^\dagger Y_u. \tag{2.13}$$

The flavour-dependent parts in (2.12) are given by

$$P = Y_e^\dagger Y_e + Y_\nu^\dagger Y_\nu. \tag{2.14}$$

The contribution of the Y_e-dependent part in P to the running enhancement factors of angles is generally negligible. In the analysis below we will ignore it and take $P \approx Y_\nu^\dagger Y_\nu$. Later reference to specific factors will be made *in situ*.

3. RGE Running of Neutrino Masses & Mixing Angles

3.1. **Low Energy Parametrization.** In the MSSM the seesaw mechanism (2.4) is slightly modified:

$$m_\nu = \frac{v^2 \sin^2\beta}{2} Y_\nu^T M^{-1} Y_\nu, \tag{3.1}$$

where $\tan\beta = v_2/v_1$ is the ratio of the expectation values of the two Higgs doublet superfields $\mathbb{h}_1$ and $\mathbb{h}_2$ of the MSSM and $v = 174\,\text{GeV} = \sqrt{v_1 + v_2}$.

The seesaw mechanism can be rewritten [16] as

$$R \equiv (M^D)^{-1/2} Y_\nu U (m_\nu^D)^{-1/2} v \sin\beta, \tag{3.2}$$

where $RR^T = 1$, and M^D and m_ν^D are the diagonalized mass matrices.

From equation (3.2), the neutrino Yukawa matrix can be parametrized in terms of an arbitrary complex orthogonal matrix R:

$$Y_\nu = \frac{\sqrt{M^D} R \sqrt{m_\nu^D} U^\dagger}{v \sin\beta}; \tag{3.3}$$

The matrix R is parametrized in terms of *complex* angles θ_1, θ_2 and θ_3 :

$$R = \begin{pmatrix} c_1 c_2 & s_1 c_2 & s_2 \\ -c_3 s_1 - s_3 s_2 c_1 & c_3 c_1 - s_3 s_2 s_1 & s_3 c_2 \\ s_3 s_1 - c_3 s_2 c_1 & -s_3 c_1 - c_3 s_2 s_1 & c_3 c_3 \end{pmatrix}, \tag{3.4}$$

where $s_i \equiv \sin\theta_i$ and $c_i \equiv \sin\theta_i$. (Unlike in [16], the structure of R is just like that of V_{MNS} (4.3), with the exception that R lacks an explicit phase δ. Of the angles, θ_1 corresponds to θ_{12}, θ_2 to θ_{13} and θ_3 to θ_{23} in V.)

Note that as θ_i are complex, their sines and cosines can exceed 1 in absolute value, and are in general complex too.

3.2. **Initial Conditions at the Electroweak Scale.** The masses of particles and other experimental data (e.g. gauge couplings) were obtained from [17]. Unless otherwise indicated, we take $\tan\beta = 5$. Values for experimentally undetermined neutrino parameters were generated randomly.

The atmospheric mass squared difference was taken to be $\Delta m^2_{\rm atm} = 2.6 \times 10^{-3}\,{\rm eV}^2$ with $\tan\theta_{23} = 0.97$, the solar mass squared difference $\Delta m^2_{\rm sol} = 8.2 \times\ {\rm eV}^2$ with $\tan^2\theta_{12} = 0.39$, and $\sin\theta_{13} = 0.05$. (Thus at the electroweak scale, the atmospheric mixing angle $\theta_{23} = 44.1^\circ$, the solar mixing angle $\theta_{12} = 32.0^\circ$, and $\theta_{13} = 2.9^\circ$.) For a normal hierarchy (n.h.), m_1 was generated randomly in the range of $10^{-7}\ldots 10^{-1}\,{\rm eV}$. From m_1, m_2 and m_3 were calculated according to $m_2 = \sqrt{m_1^2 + \Delta m^2_{\rm sol}}$, and $m_3 = \sqrt{m_2^2 + \Delta m^2_{\rm atm}}$.

In case of an inverse hierarchy (i.h.), m_3 was generated in the same range, $m_1 = \sqrt{m_3^2 + \Delta m^2_{\rm atm}}$, and $m_2 = \sqrt{m_1^2 + \Delta m^2_{\rm sol}}$.

The CP-violating phases δ, $\phi_1/2$, and $\phi_2/2$ of the mixing matrix (see (4.2) and (4.3)) were in the range of $0\ldots 2\pi$.

The magnitudes and phases of the complex angles θ_1, θ_2, and θ_3 of the orthogonal matrix R in the parametrization of Y_ν were in the range of $10^{-4}\ldots 10^{1.2}$ and $0\ldots 2\pi$, respectively.

The mass of the lightest neutrino singlet M_1 was in the range of $10^5\ldots 10^{15}\,{\rm GeV}$, the mass of the second singlet $M_2 \in M_1\ldots 10^{15.5}\,{\rm GeV}$, and the mass of the heaviest singlet $M_3 \in M_2\ldots 10^{16}\,{\rm GeV}$.

3.3. **Running of RGEs.** We developed a *Mathematica*™ 5 program to model the renormalization group running from the low energy electroweak scale to the high energy GUT scale.

In each energy interval between the electroweak scale and the GUT scale, divided into four by heavy mass eigenvalues, the RGEs for the effective coupling κ_{gf} (2.9), the singlet neutrino Yukawa matrix Y_ν (2.10), and the singlet mass matrix M (2.11) together with the RGEs

for the gauge and other Yukawa couplings are solved numerically. At thresholds, the effective theories were matched as described below.

3.4. **Matching of κ, Y_ν, and M.** Below M_1, the lowest threshold, the heavy neutrino Yukawa matrix Y_ν and heavy neutrino mass matrix M are zero. At M_1, the first element, M_{11}, on the main diagonal of M is set to M_1 (giving $\overset{(1)}{M}$). Then the first line of Y_ν is calculated from (3.3) (giving $\overset{(1)}{Y_\nu}$), and κ below M_1 is matched to $\overset{(1)}{\kappa}$ above M_1 according to (2.6): $\overset{(1)}{\kappa} = \kappa - 2\overset{(1)}{Y_\nu^T}\overset{(1)}{M_n^{(-1)}}\overset{(1)}{Y_\nu}$.

At next thresholds, the procedure is repeated. Note that in general, instead of $\overset{(n-1)}{\kappa}$ the combination (2.7) with $\overset{(n-1)}{\kappa}$, $\overset{(n-1)}{M}$ and $\overset{(n-1)}{Y_\nu}$ has to be used in formulae for calculating $U_{\rm MNS}$ and masses at M_n.

As the matrix R in the parametrization of Y_ν is defined via Y_ν, M, and $m_\nu \propto \kappa$, all of which evolve through RG running, it has to be recalculated at M_2 and M_3. We calculate an "$\overset{(n)}{R}$" by substituting RGE-run $\overset{(n-1)}{Y_\nu}$, $\overset{(n-1)}{M}$ and $\overset{(n-1)}{\kappa}$ into (3.2) at M_n. Next, from the $\overset{(n)}{R}$ the complex angles θ_1, θ_2, and θ_3 are extracted, and substituted into (3.4) to calculate the new R.

4. Neutrino Mixing Parameters

4.1. **Definition of the Mixing Matrix.** The neutrino mixing matrix $U_{\rm MNS}$ transforms the neutrino mass eigenstates into flavour eigenstates:

$$\begin{pmatrix} \nu_{e\rm L} \\ \nu_{\mu\rm L} \\ \nu_{\tau\rm L} \end{pmatrix} = \begin{pmatrix} U_{e1} & U_{e2} & U_{e3} \\ U_{\mu1} & U_{\mu2} & U_{\mu3} \\ U_{\tau1} & U_{\tau2} & U_{\tau3} \end{pmatrix} \begin{pmatrix} \nu_{1\rm L} \\ \nu_{2\rm L} \\ \nu_{3\rm L} \end{pmatrix}. \tag{4.1}$$

The mixing matrix is parametrized as

$$U_{\rm MNS} = {\rm diag}(e^{i\delta_e}, e^{i\delta_\mu}, e^{i\delta_\tau}) \cdot V_{\rm MNS} \cdot {\rm diag}(e^{-i\phi_1/2}, e^{\phi_2/2}, 1), \tag{4.2}$$

where

$$V_{\rm MNS} = \begin{pmatrix} c_{12}c_{13} & s_{12}c_{13} & s_{13}e^{-i\delta} \\ -c_{23}s_{12} - s_{23}s_{13}c_{12}e^{i\delta} & c_{23}c_{12} - s_{23}s_{13}s_{12}e^{i\delta} & s_{23}c_{13} \\ s_{23}s_{12} - c_{23}s_{13}c_{12}e^{i\delta} & -s_{23}c_{12} - c_{23}s_{13}s_{12}e^{i\delta} & c_{23}c_{23} \end{pmatrix} \tag{4.3}$$

is the Maki-Nakagawa-Sakata (MNS) matrix, the lepton sector analogue of the Cabibbo-Kobayashi-Maskawa (CKM) quark mixing matrix. In the mixing matrix $s_{ij} \equiv \sin\theta_{ij}$ and $c_{ij} \equiv \sin\theta_{ij}$, respectively.

The phases δ_e, δ_μ, and δ_τ are unphysical, as they can be removed by a phase rotation of the neutrino fields.

The matrix $U_{\rm MNS}$ diagonalizes the effective neutrino mass matrix m_ν in the basis where $Y_e^\dagger Y_e = {\rm diag}(y_e^2, y_\mu^2, y_\tau^2)$, that is,

$$U^T m_\nu U = {\rm diag}(m_1, m_2, m_3). \tag{4.4}$$

(Equivalently, neutrino masses are square roots of the eigenvalues of $m_\nu m_\nu^\dagger$.)

Neutrino masses m_i are positive, with $m_1 < m_2 < m_3$ for normal hierarchy, and $m_3 < m_1 < m_2$ for inverse hierarchy.

4.2. **Extraction of Parameters.** In the standard (LMA) parametrization, the mixing angles θ_{13} and θ_{23} lie in the interval $0 \ldots \pi/2$. By reordering the masses, θ_{12} can be restricted to $0 \leq \theta_{12} \leq \pi/4$. – In the solar mass difference $\Delta m^2_{\text{sol}} = m_i^2 - m_j^2$ the mass labels $i, j \neq 3$ by convention, while in $\Delta m^2_{\text{atm}} = m_k^2 - m_l^2$ either k or l equals 3. Once the mass label 3 is fixed, the label 2 is given to the eigenvector of the remaining two that has the lower modulus of the first component to ensure that $\theta_{12} < \pi/4$ [18].

However, in order to show the change of mass hierarchy more pictorially, we chose to reorder the masses to the same mass hierarchy (normal or inverted) as at the electroweak scale, allowing θ_{12} in the same range as the other angles. (For example, if m_1 and m_2 change places, $\cos\theta_{12}$ changes place with $\sin\theta_{12}$ in the mixing matrix, so that $\theta_{12} \to \pi/2 - \theta_{12}$. See section 7 for full discussion.)

To calculate the mixing angles, the following formulae were used:

$$\theta_{12} = \begin{cases} \arctan \frac{|U_{12}|}{|U_{11}|} & \text{if } U_{11} \neq 0, \\ \frac{\pi}{2} & \text{else,} \end{cases} \tag{4.5a}$$

$$\theta_{13} = \arcsin |U_{13}|, \tag{4.5b}$$

$$\theta_{23} = \begin{cases} \arctan \frac{|U_{23}|}{|U_{33}|} & \text{if } U_{33} \neq 0, \\ \frac{\pi}{2} & \text{else.} \end{cases} \tag{4.5c}$$

The neutrino masses and mixing angles were calculated from U_{MNS} with the `MixingParameterTools` package by Antusch *et al.* [14]. At the GUT scale, neutrino masses and columns of the mixing matrix were reordered according to the hierarchy chosen at the electroweak scale as described above, if needed, and mixing angles recalculated.

5. Results

We studied neutrino mass matrices evaluated from the electroweak to the GUT scale with various initial values of the complex orthogonal matrix R in the parametrization (3.3) of Y_ν. We investigated the following cases for both the normal and inverse hierarchy of neutrino masses at the electroweak scale:

(1) $R = \mathbb{1}$, or $\theta_1 = \theta_2 = \theta_3 = 0$

(2) a random θ_i, and $\theta_{j\neq i} = 0$ with $i, j \in \{1, 2, 3\}$

(3) random orthogonal R, or all angles θ_i random.

The RGEs were evaluated many times with randomly varying initial conditions (see section 3.2). The mixing angles at the GUT scale were plotted against parametres at the electroweak scale. On the plots, the light neutrino masses m_1 and m_3 are in eV, the heavy singlet masses in GeV. Mixing angles are shown in degrees.

The light grey color signifies θ_{12}, the darker gray θ_{23}, and the darkest grey θ_{13}.

5.1. **Normal Hierarchy with Unit R.** In the case of $R = \mathbb{1}$, the mixing angles do not run, except for θ_{12} in the region of nearly degenerate neutrino masses around 0.1 eV. For a larger $\tan\beta$, the running of θ_{12} for near-degenerate masses is larger, but in the hierarchical region the angle is not affected (not shown).

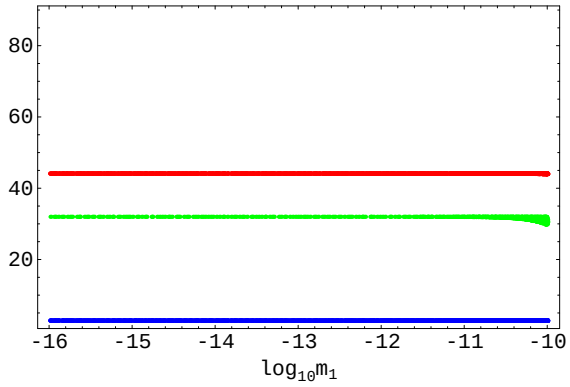

Figure 1. The mixing angles *vs.* $\log m_1$ (n.h., $R = \mathbb{1}$).

5.2. **Normal Hierarchy with Random θ_1.** In the case of random θ_1, the only mixing angle with significant running is θ_{12}, except for a few stray points of θ_{13}. The running of θ_{12} is large for near-degenerate neutrino masses. Large M_1 and M_2 enhance running of θ_{12}.

The appearance of θ_{12} above 45° indicates crossing of m_1 and m_2 (running of $\Delta m^2_{\rm sol}$ through zero), as on rearranging the masses into normal hierarchy $\cos\theta_{12}$ changes place with $\sin\theta_{12}$ in the mixing matrix, so that $\theta_{12} \to \pi/2 - \theta_{12}$.

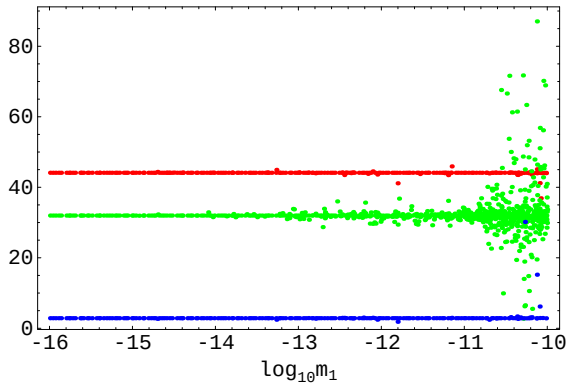

FIGURE 2. The mixing angles *vs.* $\log m_1$ (n.h., random θ_1).

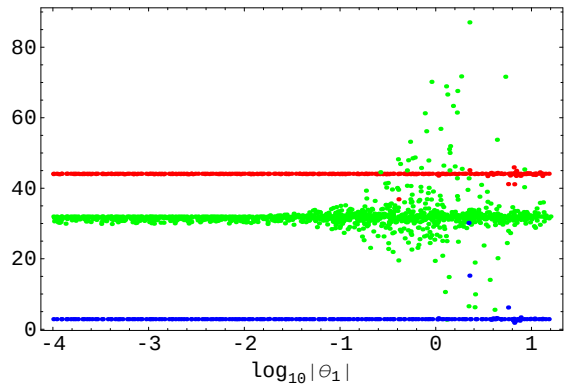

FIGURE 3. The mixing angles *vs.* $\log|\theta_1|$ (n.h., random θ_1).

5.3. **Normal Hierarchy with Random θ_2.** A random θ_2 does not influence the running of the solar mixing angle θ_{12}, as it is the same as in the case of $R = \mathbb{1}$. For near degenerate masses, large θ_2, M_2, and M_3, there occurs crossing of m_1 and m_2.

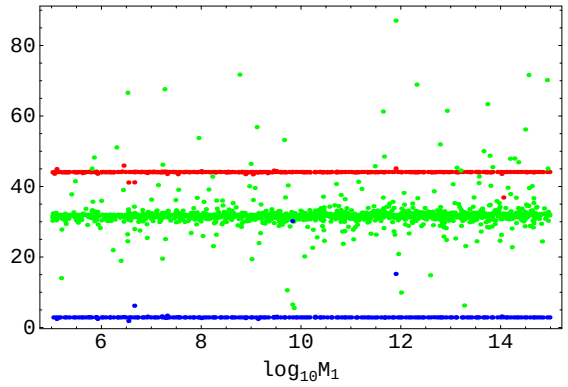

FIGURE 4. The mixing angles *vs.* $\log M_1$ (n.h., random θ_1).

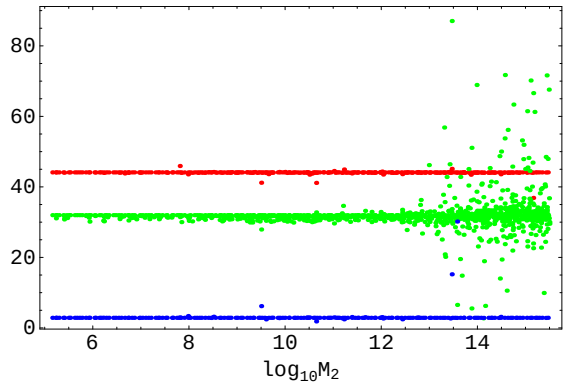

FIGURE 5. The mixing angles *vs.* $\log M_2$ (n.h., random θ_1).

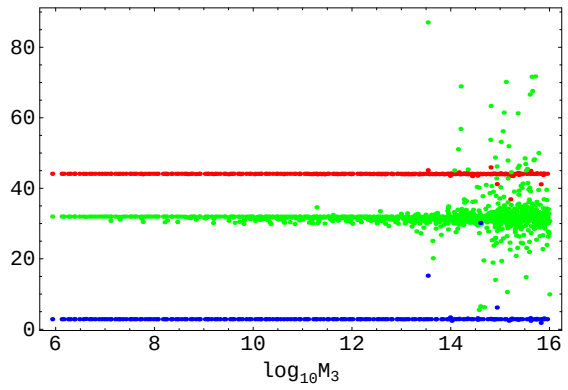

FIGURE 6. The mixing angles *vs.* $\log M_3$ (n.h., random θ_1).

In contrast, the angles θ_{13} and θ_{23} run significantly in the case of near-degenerate masses.

5.4. **Normal Hierarchy with Random θ_3.** For random θ_3, the significant running of the angles θ_{13} and θ_{23} does not depend on light

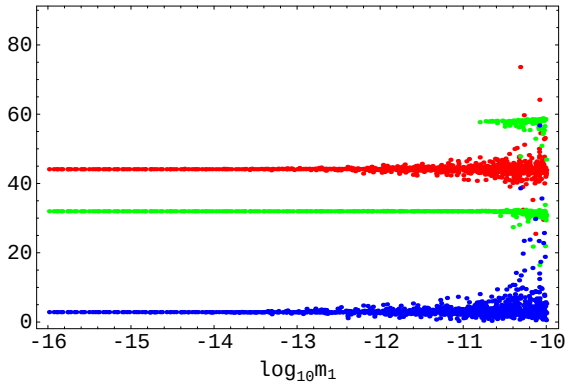

FIGURE 7. The mixing angles *vs.* $\log m_1$ (n.h., random θ_2).

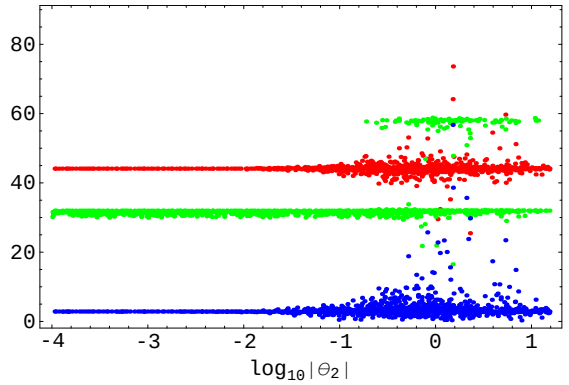

FIGURE 8. The mixing angles *vs.* $\log|\theta_2|$ (n.h., random θ_2).

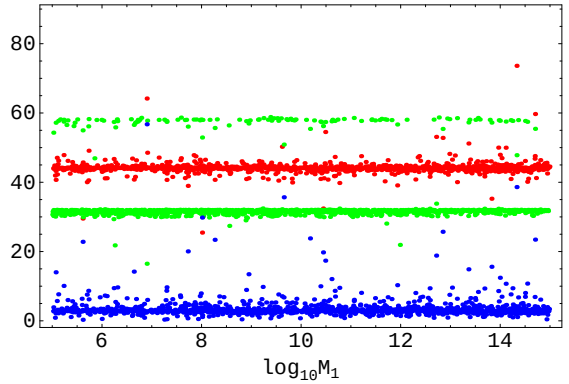

FIGURE 9. The mixing angles *vs.* $\log M_1$ (n.h., random θ_2).

neutrino masses (except for a few points in the case of very degenerate masses), but is larger when the singlet masses M_2 and M_3 are high. The running of θ_{12} is the same as for $R = \mathbb{1}$.

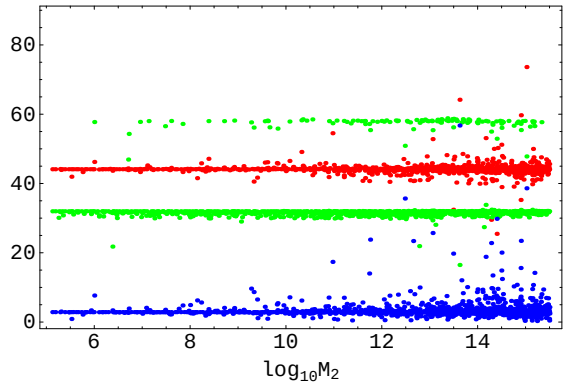

FIGURE 10. The mixing angles *vs.* $\log M_2$ (n.h., random θ_2).

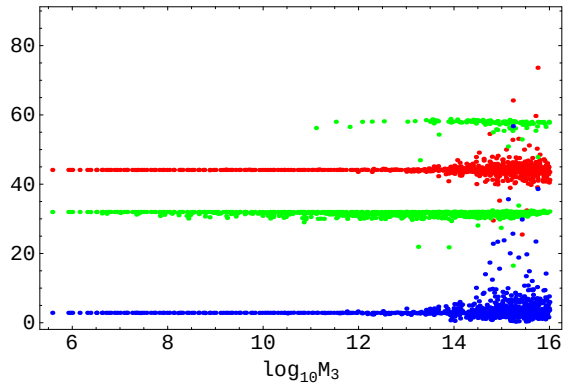

FIGURE 11. The mixing angles *vs.* $\log M_3$ (n.h., random θ_2).

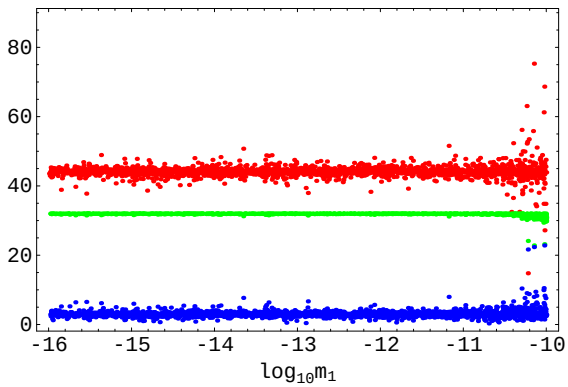

FIGURE 12. The mixing angles *vs.* $\log m_1$ (n.h., random θ_3).

5.5. **Normal Hierarchy with Random R.** If all of θ_1, θ_2, and θ_3 are random, the dependencies of the mixing angles on the initial conditions are roughly the same as would be for the sum of individual random θ_i runnings, but the running is larger for all mixing angles as compared

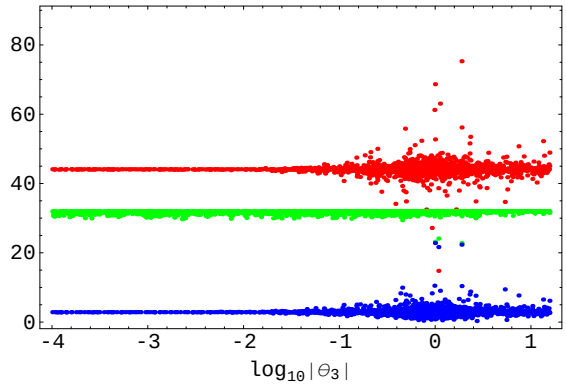

FIGURE 13. The mixing angles *vs.* $\log|\theta_3|$ (n.h., random θ_3).

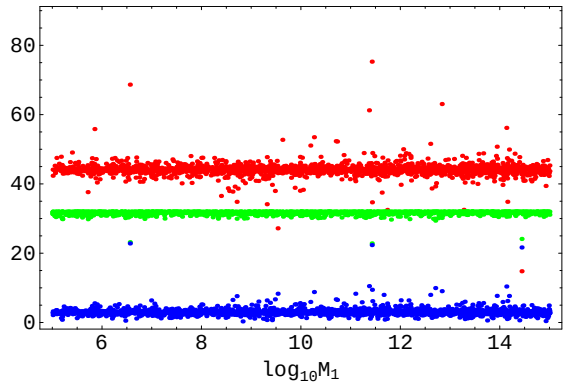

FIGURE 14. The mixing angles *vs.* $\log M_1$ (n.h., random θ_3).

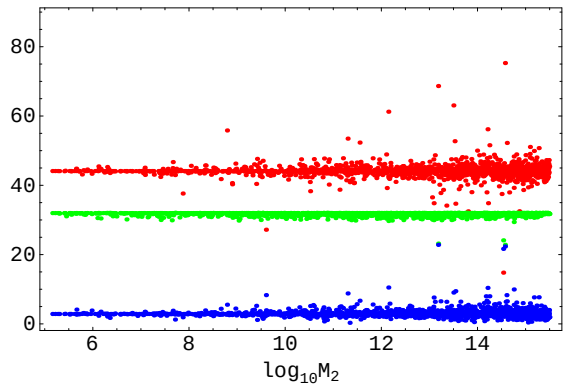

FIGURE 15. The mixing angles *vs.* $\log M_2$ (n.h., random θ_3).

with separately varying the complex angles in R. There is a relatively large percentage of crossings of m_1 and m_2.

5.6. **Inverse Hierarchy with Unit R.** For an inverse hierarchy with $R = \mathbb{1}$, the picture is very similar to that of normal hierarchy, with the

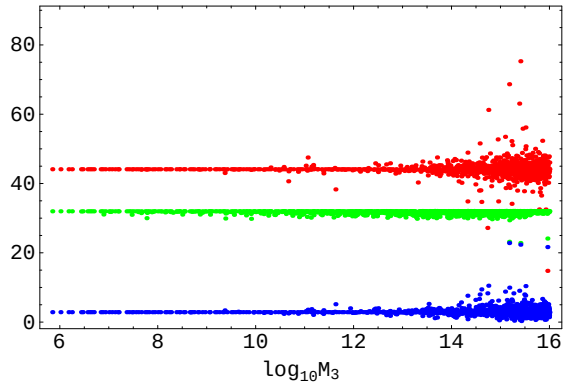

FIGURE 16. The mixing angles *vs.* $\log M_3$ (n.h., random θ_3).

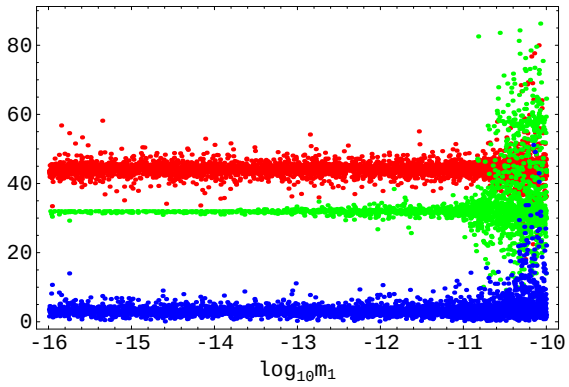

FIGURE 17. The mixing angles *vs.* $\log m_1$ (n.h., random R).

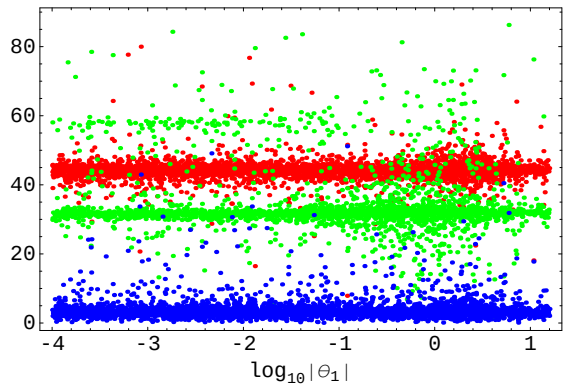

FIGURE 18. The mixing angles *vs.* $\log|\theta_1|$ (n.h., random R).

exception of several mass crossings in the region of nearly degenerate masses.

5.7. **Inverse Hierarchy with Unit R for $\tan\beta = 10$.** In the case of an inverse hierarchy with $R = \mathbb{1}$ and a larger $\tan\beta$, the running of θ_{12}

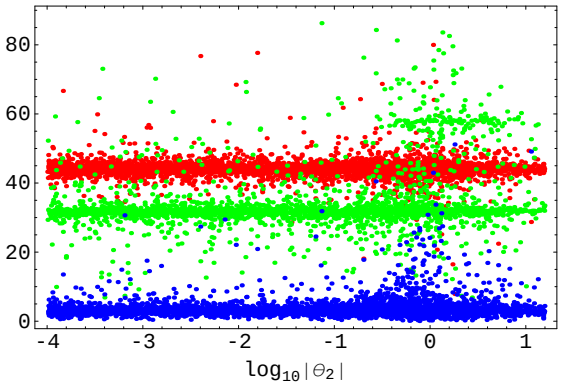

FIGURE 19. The mixing angles *vs.* $\log|\theta_2|$ (n.h., random R).

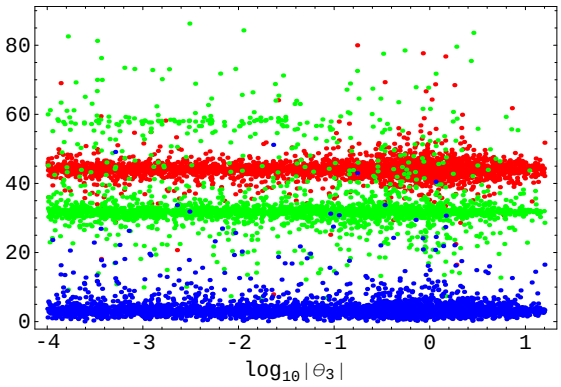

FIGURE 20. The mixing angles *vs.* $\log|\theta_3|$ (n.h., random R).

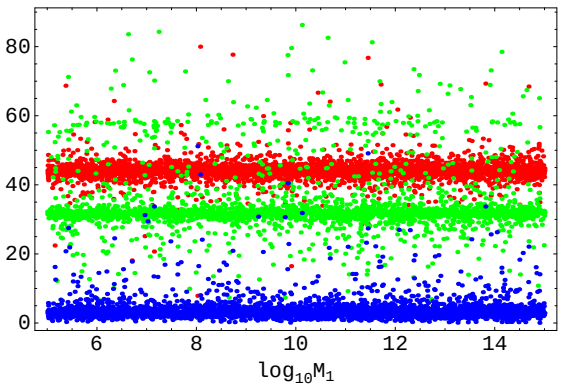

FIGURE 21. The mixing angles *vs.* $\log M_1$ (n.h., random R).

is enhanced, especially for near-degenerate masses, yet the other angles are unaffected, but for the widening of the crossed mass θ_{13} band.

5.8. **Inverse Hierarchy with Random θ_1.** A θ_1 on the order of 1 generally effects a very large running of θ_{12} and crossing of m_1 and m_2

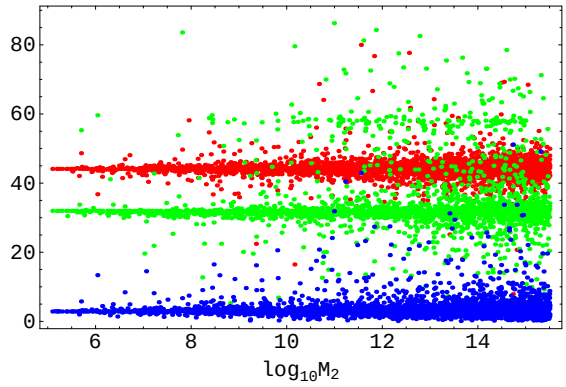

FIGURE 22. The mixing angles *vs.* $\log M_2$ (n.h., random R).

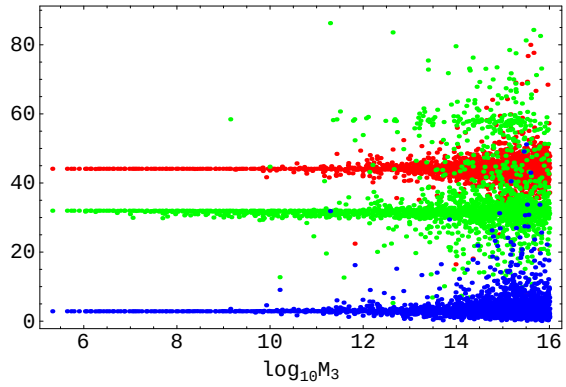

FIGURE 23. The mixing angles *vs.* $\log M_3$ (n.h., random R).

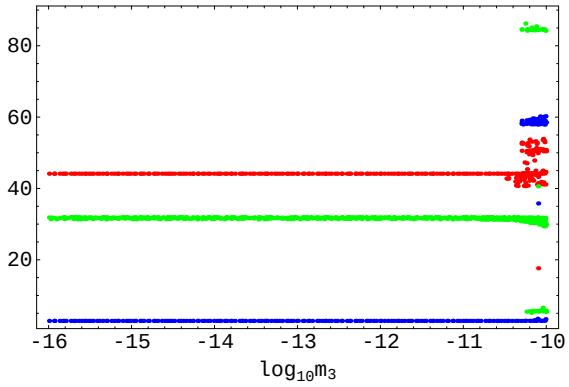

FIGURE 24. The mixing angles *vs.* $\log m_3$ (i.h., $R = \mathbb{1}$).

that are independent of neutrino masses. The other angles do not run, except for the case of nearly degenerate masses, where also notable mass crossings occur (with the same structure as for i.h. and $R = \mathbb{1}$). The running of angles and crossing of masses is significantly enhanced in the region of large M_2 and especially M_3.

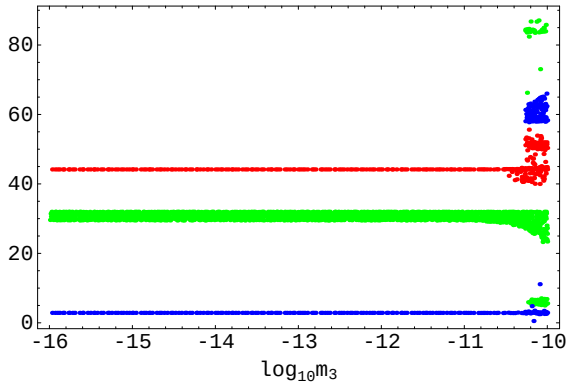

FIGURE 25. The mixing angles *vs.* $\log m_3$ (i.h., $R = \mathbb{1}$, $\tan\beta = 10$).

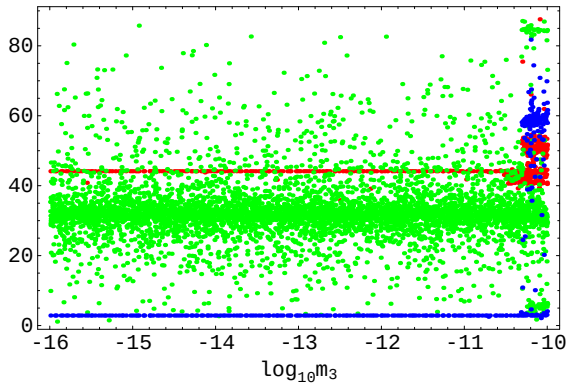

FIGURE 26. The mixing angles *vs.* $\log m_3$ (i.h., random θ_1).

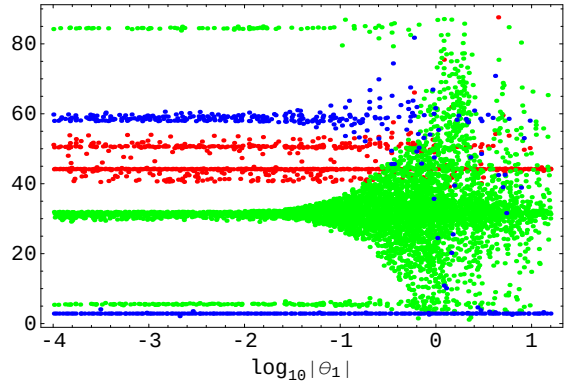

FIGURE 27. The mixing angles *vs.* $\log|\theta_1|$ (i.h., random θ_1).

5.9. **Inverse Hierarchy with Random θ_2.** For random θ_2, there is little running except for near-degenerate masses where θ_{13} runs significantly and several crossings occur.

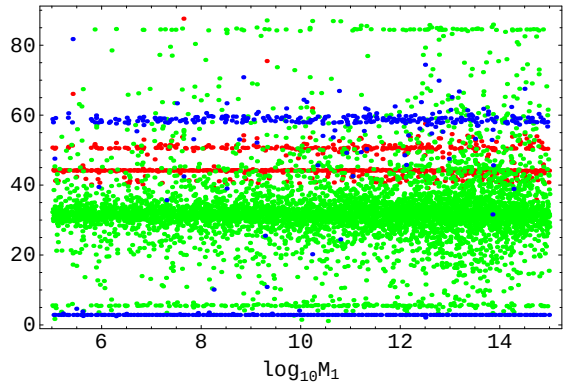

FIGURE 28. The mixing angles *vs.* $\log M_1$ (i.h., random θ_1).

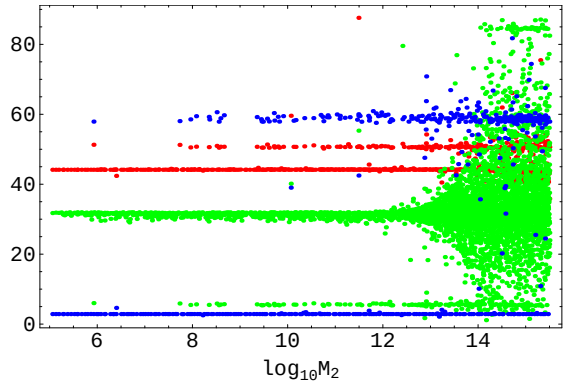

FIGURE 29. The mixing angles *vs.* $\log M_2$ (i.h., random θ_1).

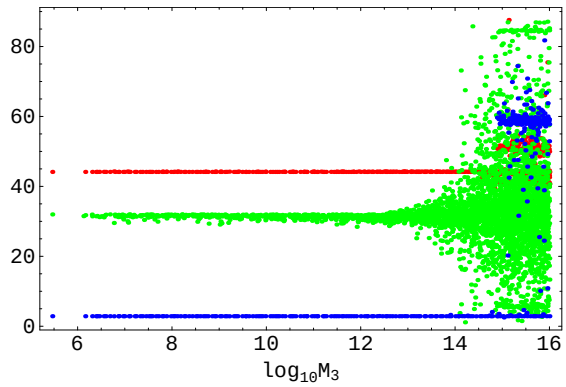

FIGURE 30. The mixing angles *vs.* $\log M_3$ (i.h., random θ_1).

5.10. **Inverse Hierarchy with Random θ_3.** In the case of random θ_3, their is some running of θ_{23} independent of masses, and several mass crossings (that occur mostly for *smaller* values of $|\theta_3|$). In the region of near-degenerate masses all angles run, but θ_{23} runs the most.

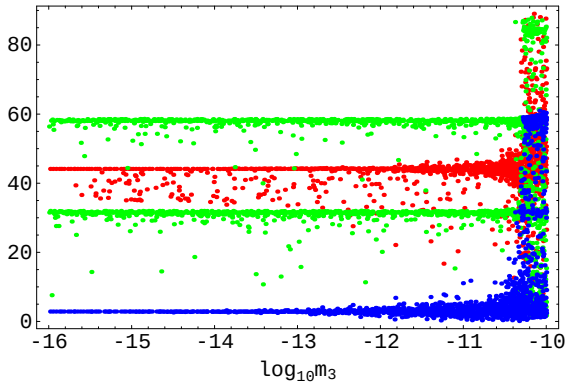

FIGURE 31. The mixing angles *vs.* $\log m_3$ (i.h., random θ_2).

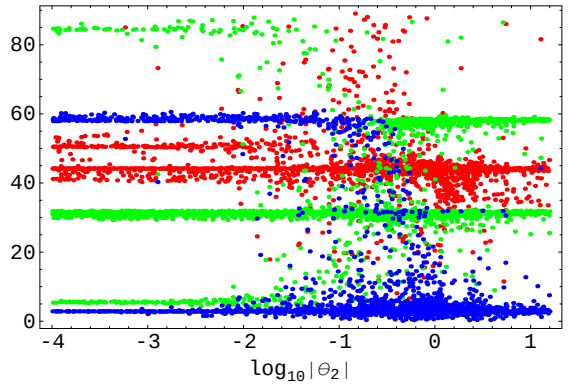

FIGURE 32. The mixing angles *vs.* $\log|\theta_2|$ (i.h., random θ_2).

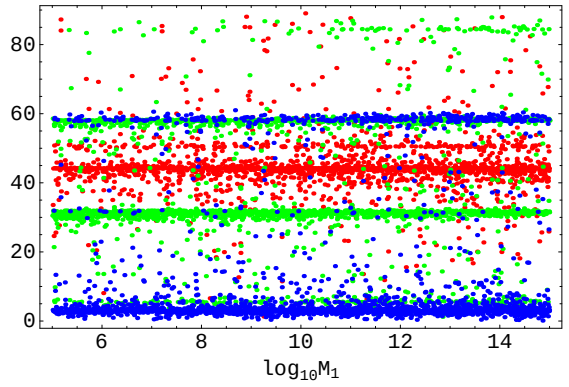

FIGURE 33. The mixing angles *vs.* $\log M_1$ (i.h., random θ_2).

5.11. **Inverse Hierarchy with Random** R**.** As for the normal hierarchy, the outcome of all of θ_1, θ_2, and θ_3 being random is roughly the same as would be if the separate θ_i runnings were combined.

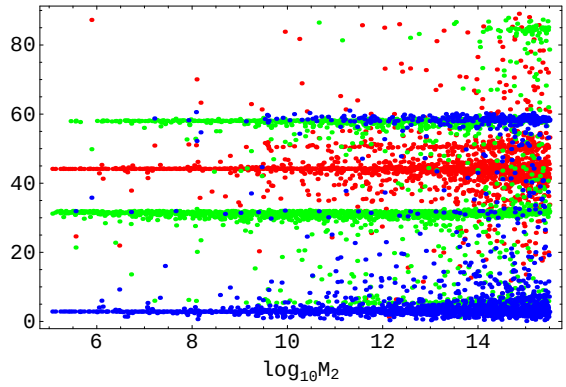

FIGURE 34. The mixing angles *vs.* $\log M_2$ (i.h., random θ_2).

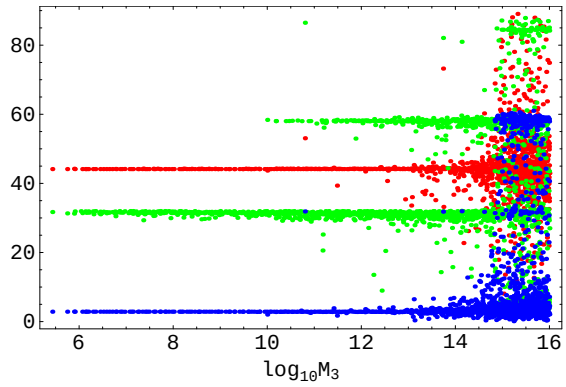

FIGURE 35. The mixing angles *vs.* $\log M_3$ (i.h., random θ_2).

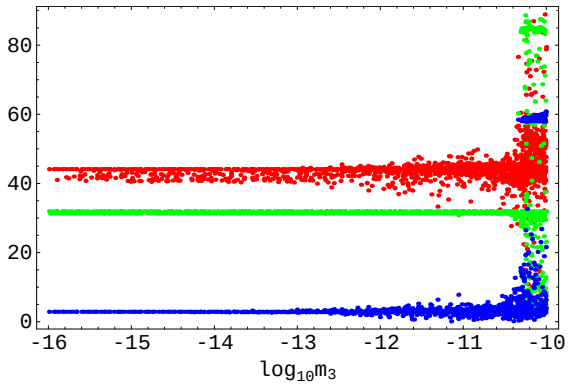

FIGURE 36. The mixing angles *vs.* $\log m_3$ (i.h., random θ_3).

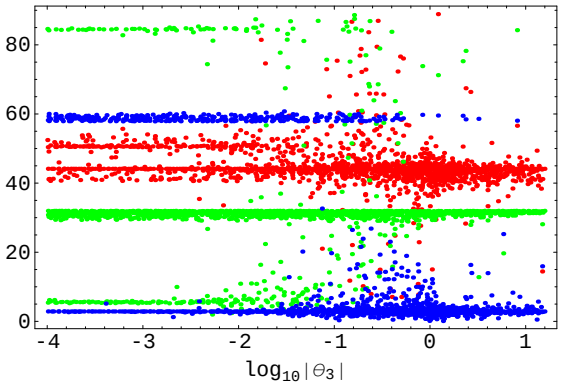

FIGURE 37. The mixing angles *vs.* $\log|\theta_3|$ (i.h., random θ_3).

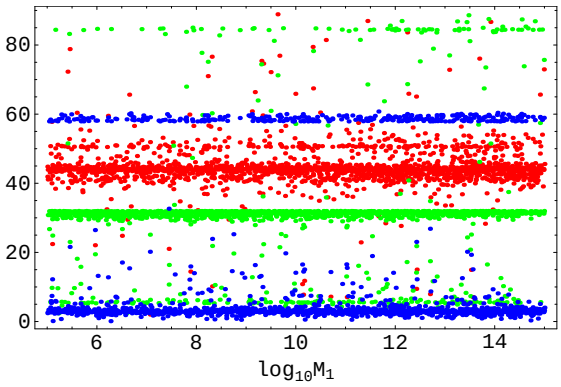

FIGURE 38. The mixing angles *vs.* $\log M_1$ (i.h., random θ_3).

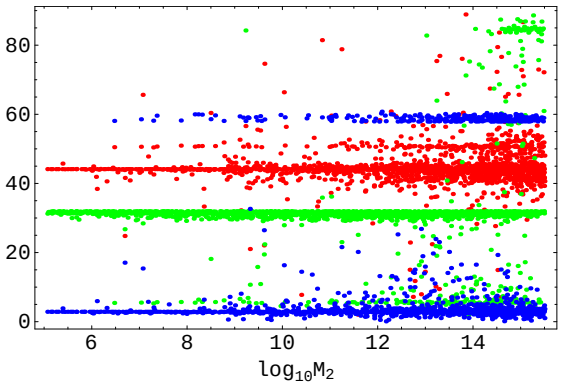

FIGURE 39. The mixing angles *vs.* $\log M_2$ (i.h., random θ_3).

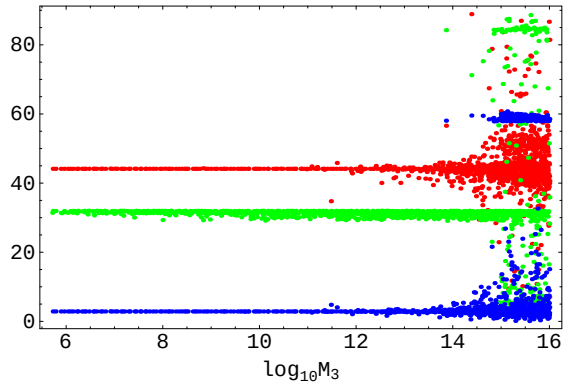

FIGURE 40. The mixing angles *vs.* $\log M_3$ (i.h., random θ_3).

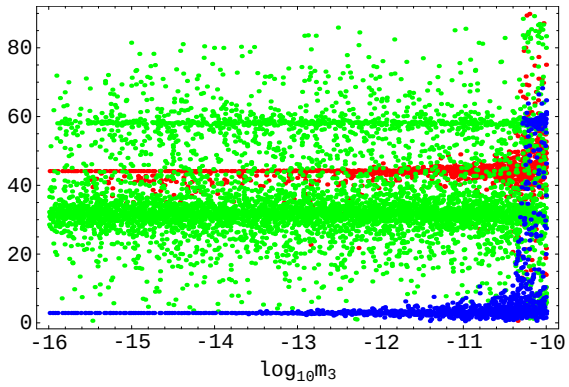

FIGURE 41. The mixing angles *vs.* $\log m_3$ (i.h., random R).

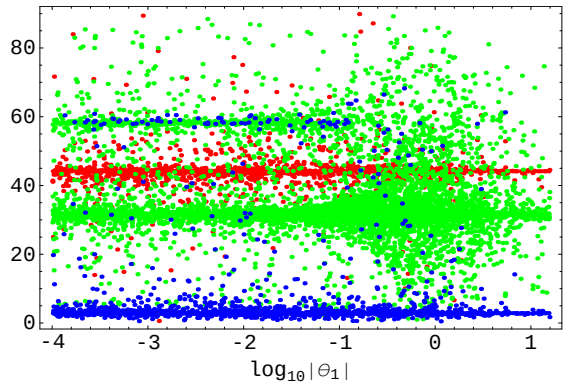

FIGURE 42. The mixing angles *vs.* $\log|\theta_1|$ (i.h., random R).

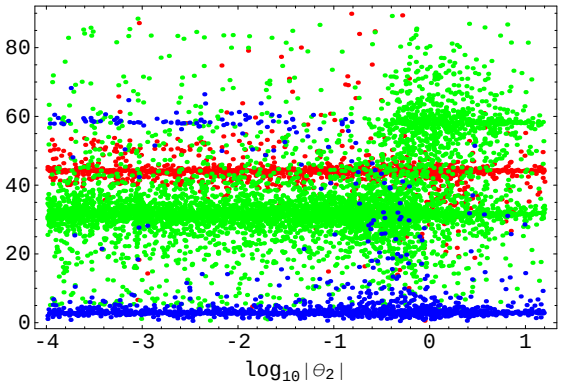

FIGURE 43. The mixing angles *vs.* $\log|\theta_2|$ (i.h., random R).

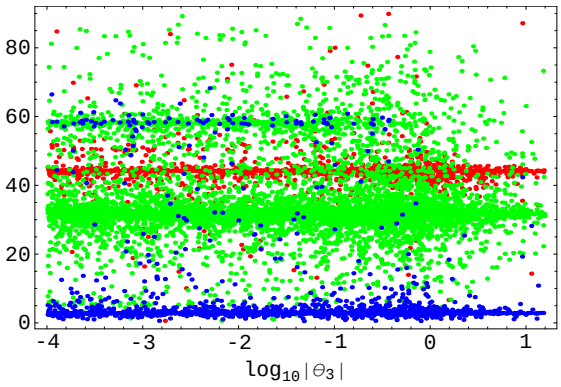

FIGURE 44. The mixing angles *vs.* $\log|\theta_3|$ (i.h., random R).

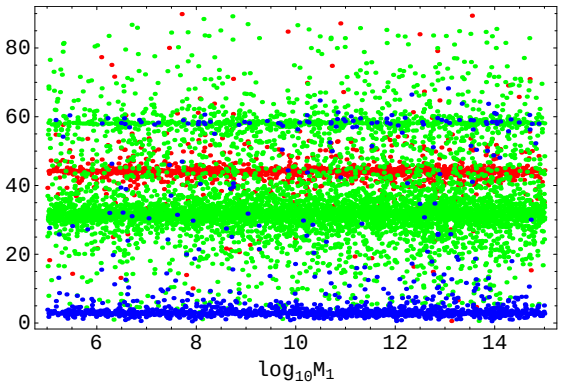

FIGURE 45. The mixing angles *vs.* $\log M_1$ (i.h., random R).

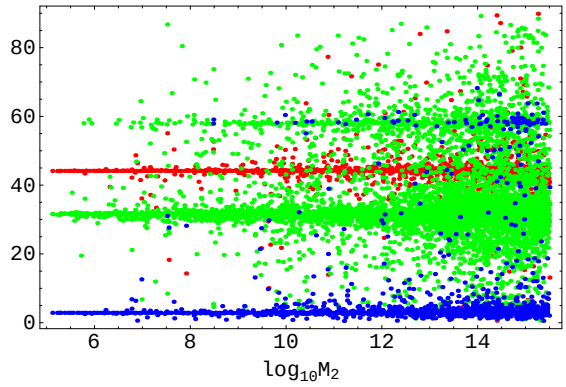

FIGURE 46. The mixing angles *vs.* $\log M_2$ (i.h., random R).

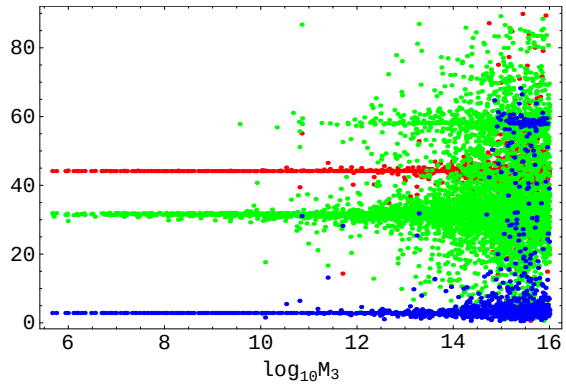

FIGURE 47. The mixing angles *vs.* $\log M_3$ (i.h., random R).

6. Comparison with Analytical Approximations

The numerical results described in section 5 were compared to analytical approximations developed in [14]. In general, the numerical and analytical results were in good agreement.

In general, as

$$\Delta\theta_{12} \propto \frac{1}{\Delta m^2_{\rm sol}}, \tag{6.1}$$

and

$$\Delta\theta_{13}, \Delta\theta_{23} \propto \frac{1}{\Delta m^2_{\rm atm}}, \tag{6.2}$$

the former angle should show larger running than the latter, which was indeed the case.

As the enhancement factors are one or two orders larger for nearly degenerate neutrinos, the latter do exhibit greater running. The same argument applies for an inverse hierarchy *vs.* a normal hierarchy.

The enhancement factors are roughly proportional to the singlet masses, and indeed it was found that two large masses M_2 and M_3 are required in order to have large running of the mixing angles, whereas the smaller M_1 is virtually uncorrelated to changes in the mixing angles.

7. Mass Crossings

In some cases, e.g. if the initial neutrino masses are almost degenerate, the squared neutrino mass differences $\Delta m^2_{\rm sol}$ or $\Delta m^2_{\rm atm}$ can run through zero, bringing about a change in mass hierarchy or mass crossing. If one insists on keeping the initial neutrino mass hierarchy at the GUT scale, and reorders the RGE-evolved masses, the columns of the neutrino mixing matrix $U_{\rm MNS}$ – that is, the eigenvectors of m'_ν – get reordered as well. As a result, on the plots of the mixing angles appear discontinous bands. (In fact, it suffices to consider $V_{\rm MNS}$ (4.3) only, as the additional phases of $U_{\rm MNS}$ do not affect the mixing angles calculated from it:

(7.1)
$$V_{\rm MNS} = \begin{pmatrix} c_{12}c_{13} & s_{12}c_{13} & s_{13}e^{-i\delta} \\ -c_{23}s_{12} - s_{23}s_{13}c_{12}e^{i\delta} & c_{23}c_{12} - s_{23}s_{13}s_{12}e^{i\delta} & s_{23}c_{13} \\ s_{23}s_{12} - c_{23}s_{13}c_{12}e^{i\delta} & -s_{23}c_{12} - c_{23}s_{13}s_{12}e^{i\delta} & c_{23}c_{23} \end{pmatrix}.$$

There are six permutations $\mathscr{P}$ of the three columns of $V_{\rm MNS}$. The identity permutation is taken to be the normal order of the columns in $V_{\rm MNS}$:

(7.2)
$$\mathscr{P}_{\rm id} = \{1\ 2\ 3\}.$$

In what follows, the values of the mixing angles are taken at the electroweak scale, in order to gain a rough understanding of the placement of the magnitude of change in the mixing angles, when the columns of $V_{\rm MNS}$ are permuted.

7.1. **The Permutation** $\{2\ 1\ 3\}$**.** If the first two columns of $V_{\rm MNS}$ change places, the angle θ_{13} and θ_{23} remain unaffected. But $\cos\theta_{12}$ is swapped with $\sin\theta_{12}$ in the mixing matrix, so that

(7.3)
$$\theta_{12} \to \pi/2 - \theta_{12}.$$

On plots, it mirrors θ_{12} around the 45°-line, resulting in a $\theta'_{12} = 58.0°$ for the initial $\theta_{12} = 32.0°$.

7.2. **The Permutation** $\{1\ 3\ 2\}$**.** If the last two columns of $V_{\rm MNS}$ change places, all angles change:

$$\tan\theta'_{12} = \frac{s_{13}}{c_{12}c_{13}} \approx \frac{s_{13}}{c_{12}}, \tag{7.4a}$$

$$\sin\theta'_{13} = c_{13}s_{12} \approx s_{12}, \tag{7.4b}$$

$$\begin{aligned}\tan\theta'_{23} &= \frac{c_{23}c_{12} - s_{23}s_{13}s_{12}e^{i\delta}}{-s_{23}c_{12} - c_{23}s_{13}s_{12}e^{i\delta}} \\ &\approx \frac{c_{23}c_{12}}{s_{23}c_{12}} \\ &= \frac{c_{23}}{s_{23}} \\ &\equiv \cot\theta_{23},\end{aligned} \tag{7.4c}$$

as $c_{13} \approx 1$ for a small θ_{13}.

Therefore,

$$\theta'_{12} \approx 3.5°, \tag{7.5a}$$

$$\theta'_{13} \approx 32.0°, \tag{7.5b}$$

$$\theta'_{23} \approx 90°. \tag{7.5c}$$

7.3. **The Permutation** $\{2\ 3\ 1\}$**.** In case of the permutation $\{2\ 3\ 1\}$,

$$\tan\theta'_{12} = \frac{s_{13}}{s_{12}c_{13}} \approx \frac{s_{13}}{s_{12}}, \tag{7.6a}$$

$$\sin\theta'_{13} = c_{12}c_{13} \approx c_{12}, \tag{7.6b}$$

$$\tan\theta'_{23} = \frac{-c_{23}s_{12} - s_{23}s_{13}c_{12}e^{i\delta}}{s_{23}s_{12} - c_{23}s_{13}c_{12}e^{i\delta}} \approx \cot\theta_{23}, \tag{7.6c}$$

yielding

$$\theta'_{12} \approx 5.5°, \tag{7.7a}$$

$$\theta'_{13} \approx 58°, \tag{7.7b}$$

$$\theta'_{23} \approx 90°. \tag{7.7c}$$

Note that the approximate estimate of θ'_{23} is the same as with $\mathscr{P}_{132}$.

7.4. **The Permutation** $\{3\ 1\ 2\}$**.** In case of the permutation $\{3\ 1\ 2\}$,

$$\tan\theta'_{12} = \frac{c_{12}c_{13}}{s_{13}} \approx \frac{c_{12}}{s_{13}}, \tag{7.8a}$$

$$\sin\theta'_{13} = s_{12}c_{13} \approx s_{12}, \tag{7.8b}$$

$$\tan\theta'_{23} = \frac{c_{23}c_{12} - s_{23}s_{13}s_{12}e^{i\delta}}{-s_{23}c_{12} - c_{23}s_{13}s_{12}e^{i\delta}} \approx \cot\theta_{23}, \tag{7.8c}$$

yielding

$$\theta'_{12} \approx 87^\circ, \tag{7.9a}$$

$$\theta'_{13} \approx 58^\circ, \tag{7.9b}$$

$$\theta'_{23} \approx 90^\circ. \tag{7.9c}$$

7.5. **The Permutation** $\{3\ 2\ 1\}$**.**

$$\tan\theta'_{12} = \frac{c_{13}s_{12}}{s_{13}} \approx \frac{s_{12}}{s_{13}}, \tag{7.10a}$$

$$\sin\theta'_{13} = \sin\theta'_{13} \approx c_{12}, \tag{7.10b}$$

$$\tan\theta'_{23} = \tan\theta'_{23} \approx \cot\theta_{23}, \tag{7.10c}$$

yielding

$$\theta'_{12} \approx 87^\circ, \tag{7.11a}$$

$$\theta'_{13} \approx 58^\circ, \tag{7.11b}$$

$$\theta'_{23} \approx 90^\circ. \tag{7.11c}$$

8. Conclusions

We studied the running of low-energy neutrino mixing angles and masses to the scale of Grand Unified Theories (GUT) in the Minimal Supersymmetric Standard Model extended with three heavy neutrino singlets (the minimal supersymmetric seesaw mechanism).

The influence of a complex orthogonal matrix R in the parametrization of Y_ν to the running of neutrino parametres was studied. For a unit R, the running is generally vanishing. It was found that different complex angles in the parametrization of R enhance the running of different mixing angles, and that a non-diagonal R generally favours large running of the mixing angles.

Large M_2 and M_3 are required in order to have significant running of the mixing angles.

The running of the mixing angles is generally larger for an inverse hierarchy (i.h.) than for a normal one. Also, the neutrino masses tend to change their hierarchy more for an i.h.

In general, the running of the mixing angles was found do be in qualitative agreement with analytical approximations derived in the literature.

9. Kokkuvõte

Me uurisime neutriinode massimaatriksi renormrühma jooksmist raskete singlettneutriinodega minimaalses supersümmeetrilises Standardmudelis (MSSM). Eeldasime, et raskete neutriinode massid pole kõdunud, ja seega integreeritakse välja ükshaaval.

Renormrühma võrrandite lahendamiseks kirjutasime *Mathematica*™ programmi. Alustades elektronõrgalt skaalalt, genereerisime juhuslikult need algtingimused, mis pole veel eksperimentaalselt määratud, ja renormrühma võrrandeid lahendades leidsime neutriinode parameetrid suurte ühendteooriate (GUT) skaalal. Uurisime neutriinomasside tavalist ja pöördhierarhiat.

Uurisime, millist mõju avaldab neutriinode segunemisnurkade jooksmisele raskete neutriinode Yukawa maatriksi parametriseeringus olev kompleksne ortogonaalne maatriks R.

Leidsime, et numbrilised tulemused on kvalitatiivses kooskõlas analüütiliste lähendustega [14].

Uurisime masside hierarhia muutumist ehk masside ristumist ja sellega kaasnevaid muutuseid segunemisnurkades.

10. Abstract

We study renormalization group running of neutrino mass matrix in the Minimal Supersymmetric Standard Model (MSSM) extended with heavy singlet neutrinos (the minimal supersymmetric seesaw mechanism). The heavy mass eigenvalues are assumed non-degenerate and are integrated out one at a time.

A *Mathematica*™ program to model the renormalisation group running was developed. Starting with experimentally determined boundary conditions at the electroweak scale and generating randomly the parametres not yet determined, the neutrino mixing angles are evolved to the GUT scale via renormalisation group running. Both normal and inverse mass hierarchy were under consideration.

The influence of a complex orthogonal matrix R in the parametrization of the singlet Yukawa on RG running was studied.

Numerical results for different initial conditions were found to be in a qualitative agreement with analytical approximations [14] of mixing angle running.

The hierarchy changing or crossing of masses, and the respective changes in the mixing angles were investigated.

References

[1] S. M. Bilenky and S. T. Petcov, Massive Neutrinos And Neutrino Oscillations. Rev. Mod. Phys. **59** (1987) 671 [Erratum-ibid. **61** (1989) 169].

[2] Y. Fukuda, Observation of neutrinos at Super-Kamiokande. *Prepared for 8th International Conference on Calorimetry in High-Energy Physics (CALOR 99), Lisbon, Portugal, 13-19 Jun 1999*

[3] Q. R. Ahmad *et al.* [SNO Collaboration], Direct evidence for neutrino flavor transformation from neutral-current interactions in the Sudbury Neutrino Observatory. Phys. Rev. Lett. **89**, 011301 (2002) [arXiv:nucl-ex/0204008].

[4] Q. R. Ahmad *et al.* [SNO Collaboration], Measurement of day and night neutrino energy spectra at SNO and constraints on neutrino mixing parameters. Phys. Rev. Lett. **89**, 011302 (2002) [arXiv:nucl-ex/0204009].

[5] P. Minkowski, Mu $\to$ E Gamma At A Rate Of One Out Of 1-Billion Muon Decays? Phys. Lett. B **67**, 421 (1977).

[6] T. Yanagida, Horizontal Gauge Symmetry And Masses Of Neutrinos. *In Proceedings of the Workshop on the Baryon Number of the Universe and Unified Theories, Tsukuba, Japan, 13-14 Feb 1979*

[7] S. L. Glashow, The Future Of Elementary Particle Physics. HUTP-79-A059 *Based on lectures given at Cargese Summer Inst., Cargese, France, Jul 9-29, 1979*

[8] M. Gell-Mann, P. Ramond and R. Slansky, Complex Spinors And Unified Theories. Print-80-0576 (CERN)

[9] R. N. Mohapatra and G. Senjanovic, Neutrino Masses And Mixings In Gauge Models With Spontaneous Parity Violation. Phys. Rev. D **23**, 165 (1981).

[10] S. Antusch, M. Drees, J. Kersten, M. Lindner and M. Ratz, Neutrino mass operator renormalization in two Higgs doublet models and the MSSM. Phys. Lett. B **525** (2002) 130 [arXiv:hep-ph/0110366].

[11] S. Antusch, M. Drees, J. Kersten, M. Lindner and M. Ratz, Neutrino mass operator renormalization revisited. Phys. Lett. B **519**, 238 (2001) [arXiv:hep-ph/0108005].

[12] S. Antusch, J. Kersten, M. Lindner and M. Ratz, Neutrino mass matrix running for non-degenerate see-saw scales. Phys. Lett. B **538** (2002) 87 [arXiv:hep-ph/0203233].

[13] M. Fukugita and T. Yanagida, Baryogenesis Without Grand Unification. Phys. Lett. B **174**, 45 (1986).

[14] S. Antusch, J. Kersten, M. Lindner, M. Ratz and M. A. Schmidt, Running neutrino mass parameters in see-saw scenarios. JHEP **0503** (2005) 024 [arXiv:hep-ph/0501272].

[15] P. H. Chankowski and S. Pokorski, Quantum corrections to neutrino masses and mixing angles. Int. J. Mod. Phys. A **17**, 575 (2002) [arXiv:hep-ph/0110249].

[16] J. R. Ellis, J. Hisano, S. Lola and M. Raidal, CP violation in the minimal supersymmetric seesaw model. Nucl. Phys. B **621** (2002) 208 [arXiv:hep-ph/0109125].

[17] S. Eidelman *et al.*, Phys. Lett. B **592** 1 (2004) [URL: http://pdg.lbl.gov]

[18] S. Antusch, J. Kersten, M. Lindner and M. Ratz, Running neutrino masses, mixings and CP phases: Analytical results and phenomenological consequences. Nucl. Phys. B **674** (2003) 401 [arXiv:hep-ph/0305273].